

# Colored-hadron distribution in hadron scattering in SU(2) lattice QCD

Toru T. Takahashi<sup>1</sup> and Yoshiko Kanada-En'yo<sup>2</sup>

<sup>1</sup>*Gunma National College of Technology, Maebashi, Gunma 371-8530, Japan*

<sup>2</sup>*Department of Physics, Kyoto University, Sakyo, Kyoto 606-8502, Japan*

(Dated: June 22, 2016)

In color SU(2) lattice QCD, we investigate colored-diquark distributions in two-hadron scatterings by means of Bethe-Salpeter amplitudes on the lattice. With colored-diquark operators in the Coulomb gauge, we measure components of two colored diquarks realized as intermediate states via one gluon exchange (OGE) processes in hadron scattering. From the colored-diquark distributions, we estimate the dominant range of gluon (color) exchanges between closely located two hadrons. We find that the colored-diquark components are enhanced at the short range ( $<0.2$  fm) and their tails show the single-exponential damping. In order to distinguish the genuine colored-diquark components originating in the color exchange processes from trivial colored two-quark components contained in two color-singlet hadrons as a result of simple transformation of hadronic basis, we repeat the analyses on the artificially constructed gauge fields, where low- and high-momentum gluon components are decoupled and only restricted pair of quarks can share and exchange low-momentum gluons. We observe qualitatively the same behaviors and confirm that the short-range enhancement of the colored-diquark distributions is the genuine OGE-origin color excitation in hadron scattering.

PACS numbers: 12.38.Aw, 12.38.Gc

## I. INTRODUCTION

Hadron-hadron interactions play important roles in nuclear and hadron physics. While the long- and the intermediate-range interactions are well described by one-boson-exchange potentials (OBEP) [1–4], the short-range part of the hadronic interactions has not been well clarified so far. When hadrons are located closely each other, the internal quark structures are of much importance and interactions should be described in terms of quarks and gluons. In recent lattice studies, the short-range interactions have been investigated based on QCD, the fundamental theory of the strong interaction, and especially the observed repulsive cores in the baryon interactions on the lattice are found to be consistent with the quark-model based interpretation [5–9], where the color-magnetic interactions via one gluon exchange (OGE) processes and Pauli blocking effects among quarks play an essential role for the origin of repulsive cores.

In Ref. [10], we evaluated hadron-hadron interactions in color SU(2) QCD by means of Bethe-Salpeter amplitudes on the lattice. In the previous work, three different types of hadronic interactions were actually found. One is the middle-range universal attractive force, which can be found in all the interaction channels and is independent from quark masses. It is expected to be generated by nonperturbative gluonic degrees of freedom. Second is the short-range repulsive force, for which the Pauli blocking effect and the color-magnetic interaction among quarks are essential. The last is the short-range attractive force, which is clearly seen in the four-flavor channel without the Pauli blocking effect. This short-range attraction has the strong quark-mass dependence and would be originated from gluon exchanges among quarks. As just clarified, gluon exchange is an important piece in hadron interactions besides boson exchanges.

Such gluon-exchange processes would be also important from the view point of color exchanges between hadrons. In a two-hadron scattering at a long distance, the color exchange does not occur and quarks in a color-singlet hadron are all confined. Only color-singlet objects, like mesons or glueballs, can be exchanged between hadrons. At a short distance, however, colors can be exchanged via gluon exchanges between hadrons, corresponding to the transition from two hadrons to colored many-quark objects [11–13]. The intermediate state of the two colored objects should change into two hadrons through recombination of quarks, or it gets back to the initial two-hadron channel with another color exchange. The former process corresponds to the quark exchange between two hadrons via color exchanges. Then, at the density scale where colors are actively exchanged among hadrons, quarks would freely cross among hadrons exhibiting effective quark deconfinement [14–21].

In the case of color SU(2) QCD, which we employ in the present analysis, baryons are color-singlet diquarks. Let us consider (12)(34) incoming two diquarks, where participating quarks have flavor 1, 2, 3 and 4, and 1,2- and 3,4- quark pairs form color-singlet diquarks, (12) and (34). If one gluon is exchanged between 1- and 3-quarks, it results in color exchange between 12- and 34-diquarks, and 12- and 34-diquarks get colored, forming a  $[12][34]$  two-diquark system. (Here  $[ij]$  denotes a color triplet  $ij$ -diquark.) Some possible gluon exchange processes are illustrated in Fig. 1(A)(B). These gluon exchange processes, including quark recombination processes, can be detected by probing  $[12][34]$  colored-diquark components (distribution), since any gluon exchange processes go through a  $[12][34]$  two-diquark state. However, there exist trivial colored two-quark components. (13)(24) two-diquark wavefunction contains non-zero  $[12][34]$  component as easily proved when we rewrite it in the quark

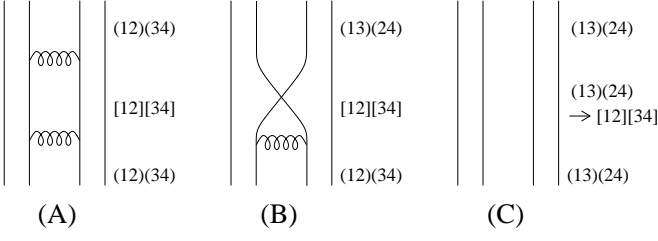


FIG. 1: (A) Incoming (12)(34) diquarks exchange colors and form outgoing (12)(34) diquarks. (B) Incoming (12)(34) diquarks exchange colors and form outgoing (13)(24) diquarks, rearranging quark pairs. (C) Incoming and outgoing diquarks are (13)(24), which however has non-zero overlap with [12][34] operator (Trivial colored two-quark component).

basis of 12- and 34- diquarks (Fig. 1(C)). We should distinguish the genuine OGE-origin colored-diquark components from such trivial contributions.

In this article, we investigate gluon (color) exchanges between closely located two hadrons with the SU(2) lattice QCD, by looking at the colored-diquark distributions between two scattering hadrons. Especially we concentrate on the color-exchange range between two hadrons to clarify the origin of the short-range attraction in the four-flavor channel free from the Pauli blocking effect. In Sec.II, the detail of our formulation is presented. The results are shown in Sec.III, and Sec.IV is devoted to the additional analysis to confirm the results. Results are discussed in Sec.V and our present study is summarized in Sec.VI.

## II. FORMULATION

We follow the strategy proposed by CP-PACS group [22, 23], where “wavefunctions” are defined as Bethe-Salpeter amplitudes measured with quark operators. We define local diquark operators  $\phi_{\{i,j\},\Gamma}^c(\mathbf{x}, t)$  as

$$\phi_{(i,j),\Gamma}(\mathbf{x}, t) \equiv \frac{1}{\sqrt{2}} \varepsilon_{ab} \Gamma_{\alpha\beta} q_i^{a\alpha}(\mathbf{x}, t) q_j^{b\beta}(\mathbf{x}, t). \quad (1)$$

for color-singlet diquarks, and as

$$\phi_{[i,j],\Gamma}^c(\mathbf{x}, t) \equiv \frac{1}{\sqrt{6}} T_{ab}^c \Gamma^{\alpha\beta} q_i^{a\alpha}(\mathbf{x}, t) q_j^{b\beta}(\mathbf{x}, t). \quad (2)$$

for color-triplet diquarks. The subscripts  $i$  and  $j$  denote quark flavors and  $(i, j)$  and  $[i, j]$  show that  $i, j$ -quark pair belongs to a color-singlet and color-triplet state, respectively.

$q_i^{a\alpha}(\mathbf{x}, t)$  is a quark operator located at  $(\mathbf{x}, t)$  that has the color index  $a$ , the spinor index  $\alpha$  and the flavor index  $i$ .  $\varepsilon_{ab}$  is an antisymmetric tensor with  $\varepsilon_{12} = 1$  and  $T_{ab}^c$  is a tensor that projects the diquark onto a color-triplet state (vector representation).  $\Gamma$  set to  $C\gamma_5$  ( $C\gamma_\mu$ ) makes a  $J = 0$  ( $J = 1$ ) diquark state.

In order to measure the relative wavefunction in diquark-diquark scattering, we compute two-diquark correlators  $W_{\{i,j\}\{k,l\}}^\Gamma(\mathbf{R}, t)$  defined as

$$W_{(i,j)(k,l)}^\Gamma(\mathbf{R}, t) \equiv \sum_{\mathbf{x}} \langle \phi_{(i,j),\Gamma}(\mathbf{x}, t) \phi_{(k,l),\Gamma}(\mathbf{x} + \mathbf{R}, t) \phi_{(i,j),\Gamma}^\dagger(\mathbf{0}, 0) \phi_{(k,l),\Gamma}^\dagger(\mathbf{0}, 0) \rangle \quad (3)$$

and

$$W_{[i,j][k,l]}^\Gamma(\mathbf{R}, t) \equiv \sum_{\mathbf{x}, c, c'} \langle \phi_{[i,j],\Gamma}^c(\mathbf{x}, t) \phi_{[k,l],\Gamma}^c(\mathbf{x} + \mathbf{R}, t) \phi_{[i,j],\Gamma}^{c'\dagger}(\mathbf{0}, 0) \phi_{[k,l],\Gamma}^{c'\dagger}(\mathbf{0}, 0) \rangle. \quad (4)$$

The summation over  $c$  and  $c'$  is taken to make the system totally color singlet.  $\mathbf{R}$  represents the relative coordinate between two scattering hadrons. Two-diquark operators are all projected to totally spin-0 states through the contraction over  $\mu$  in  $\Gamma$ . We employ wall-type operators for sources, while we use point-type operators for sinks. We hereby denote  $W_{\{i,j\}\{k,l\}}^{C\gamma_5}(\mathbf{R}, t)$  and  $W_{\{i,j\}\{k,l\}}^{C\gamma_\mu}(\mathbf{R}, t)$  as

$$\Phi_{\{i,j\}\{k,l\}S}(\mathbf{R}, t) \equiv W_{\{i,j\}\{k,l\}}^{C\gamma_5}(\mathbf{R}, t) \quad (5)$$

and

$$\Phi_{\{i,j\}\{k,l\}A}(\mathbf{R}, t) \equiv W_{\{i,j\}\{k,l\}}^{C\gamma_\mu}(\mathbf{R}, t), \quad (6)$$

throughout this paper.  $\Phi_{(i,j)(k,l)S,A}(\mathbf{R}, t)$  and  $\Phi_{[i,j][k,l]S,A}(\mathbf{R}, t)$  give color-singlet and color-triplet diquark distributions in hadron scattering. Especially, color excitation mode in hadron scattering can be probed by the color-triplet diquark distribution.

The internal wave functions of isolated diquarks probed by local quark operators are defined as

$$\begin{aligned} & \Phi_{(i,j)S,A}(\mathbf{R}, t) \\ & \equiv \sum_{\mathbf{x}} \frac{1}{\sqrt{2}} \varepsilon_{ab} \Gamma_{\alpha\beta} \langle q_i^{a\alpha}(\mathbf{x} + \mathbf{R}, t) q_j^{b\beta}(\mathbf{x}, t) \phi_{(i,j)S,A}^\dagger(\mathbf{0}, 0) \rangle. \end{aligned} \quad (7)$$

$\Gamma$  is chosen as  $C\gamma_5$  and  $C\gamma_\mu$  for scalar and axial vector diquarks,  $\Phi_{(i,j)S}$  and  $\Phi_{(i,j)A}$ , respectively.  $\mathbf{R}$  represents the relative coordinate between two quarks in the diquark.

We concentrate on S-wave scattering states of two scalar diquarks ( $\Gamma = C\gamma_5$ ), which is the ground state in  $l = 0$  channel, and we project wavefunctions  $\Phi(\mathbf{R})$  onto  $A_1^+$ -wavefunction  $\Phi(R) \equiv \Phi(|\mathbf{R}|)$ , which has overlap with  $l = 0$  states, by summing up  $\Phi(\mathbf{R})$  in terms of corresponding discrete rotations. We here neglect the contributions from  $l \geq 4$  scattering states, since such contributions can be dropped by taking large Euclidean-time separation  $t$ .

All the simulations are performed in SU(2) quenched QCD with the standard plaquette gauge action and the Wilson quark action. The lattice size is  $24^3 \times 64$  at  $\beta = 2.45$ , whose lattice spacing is about 0.1 fm if we assume  $\sqrt{\sigma}$  is 440 MeV [24, 25]. We employ four different Hopping parameters  $\kappa = 0.1450, 0.1475, 0.1500, 0.1513$  for quarks.

### III. LATTICE QCD RESULTS

#### A. Hadron masses

We show the ground-state diquark masses for each quantum number in Table I. In Fig. 2, scalar-axialvector mass splittings  $\Delta m$  are plotted as a function of the half of the axialvector diquark masses, which can be regarded as “constituent” quark masses  $m_Q$ . The dotted line denotes the fit function  $\Delta m = C/m_Q^2$ . Most of the data can be well reproduced by  $\Delta m = C/m_Q^2$ , although  $\Delta m$  at the lightest quark mass ( $m_\pi \simeq 600$  MeV) deviates from the fit function, which implies a naive quark model picture may not be valid any longer in this quark-mass region.

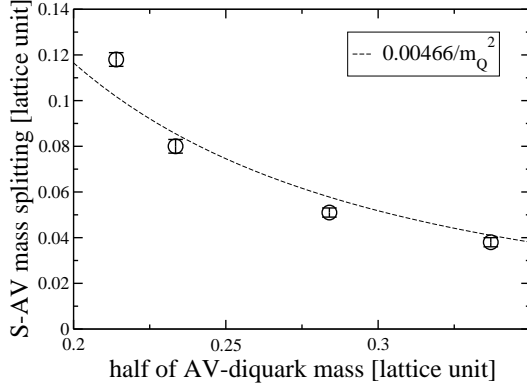


FIG. 2: Scalar-axialvector mass splitting is plotted as a function of axialvector-diquark mass. The dotted line is a fit function  $Cm_Q^{-2}$ .

$\kappa$	Scalar	Axialvector	Pseudoscalar	Vector	$\Delta m$
0.1450	0.636(2)	0.674(3)	0.893( 19)	0.897(13)	0.038(2)
0.1475	0.517(2)	0.568(4)	0.811( 28)	0.805(17)	0.051(2)
0.1500	0.387(3)	0.467(7)	0.768( 54)	0.714(24)	0.080(3)
0.1513	0.310(3)	0.428(1)	0.717(116)	0.673(30)	0.118(3)

TABLE I: All the hadronic masses are listed.  $\Delta m$  represents the scalar-axialvector diquark mass splitting.

#### B. Wavefunctions

Wavefunctions are measured from two-diquark operators for  $(1,2)(3,4)S$ ,  $[1,2][3,4]A$ ,  $(1,3)(2,4)S$ ,  $(1,3)(2,4)A$ ,  $[1,3][2,4]S$  and  $[1,3][2,4]A$  channels. Here,  $(i,j)(k,l)$  ( $[i,j][k,l]$ ) mean that  $ij$ - and  $kl$ -diquarks belong to color-singlet (color-triplet) states. Such 4-quark operators are all projected to totally color-singlet and  $J = 0$  operators. Wavefunction-analyses with  $[i,j][k,l]$  operators allow us to probe the color-excitation modes in hadron scatterings. We note that  $(1,2)(3,4)A$  and  $[1,2][3,4]S$  scattering states are prohibited, since the 12-diquark can be either  $(1,2)S$  or  $[1,2]A$  state due to the “iso-spin conservation” for 1- and 2-quarks. (The initial state is in all the cases  $(1,2)(3,4)S$  scattering state.)

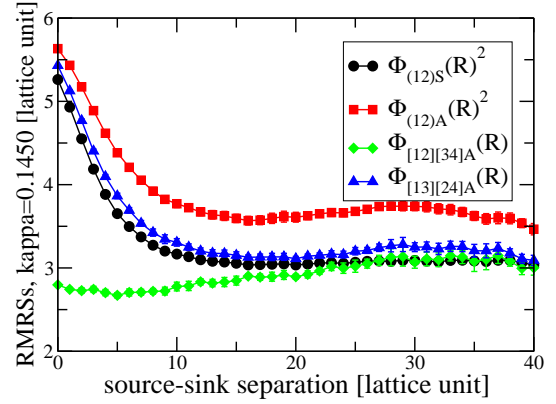


FIG. 3: The RMSRs obtained from wavefunctions  $\Phi(R, t)$  at  $\kappa = 0.1450$  are plotted as a function of a source-sink separation  $t$ . They are all normalized with  $0 \leq R \leq 7$ .

We here mention the extraction of the wavefunctions  $\Phi(R)$  using the Euclidean correlators. In Fig. 3, the RMSRs (root mean square radii) obtained from the wavefunctions  $\Phi(R, t)$  are plotted as functions of a source-sink separation  $t$ . The RMSRs are computed for  $[1,2][3,4]A$ ,  $[1,3][2,4]S$  and  $[1,3][2,4]A$  channels, in which wavefunctions show exponential damping in the asymptotic region and RMSRs can be well defined. The time-dependent wavefunctions  $\Phi(R, t)$  are all normalized with  $0 \leq R \leq 7$ , since at  $R \sim 7$  they are small enough and would be safe from finite size effects. The RMSRs evaluated from the internal wavefunctions of the scalar- and axialvector-diquarks,  $\Phi_{(12)S}$  and  $\Phi_{(12)A}$  are also displayed. They first depend on  $t$  due to excited-state contaminations, but finally show plateaus at large  $t$  region, which implies ground-state dominance. All the wavefunctions  $\Phi(R)$  are determined at  $t = 25$ ;  $\Phi(R) \equiv \Phi(R, 25)$ .

In Fig. 4, all the wavefunctions  $\Phi(R)$  are displayed as functions of the relative coordinate  $R$ . Their logarithmic plots are shown in Fig. 5. In  $(1,2)(3,4)S$ ,  $(1,3)(2,4)S$

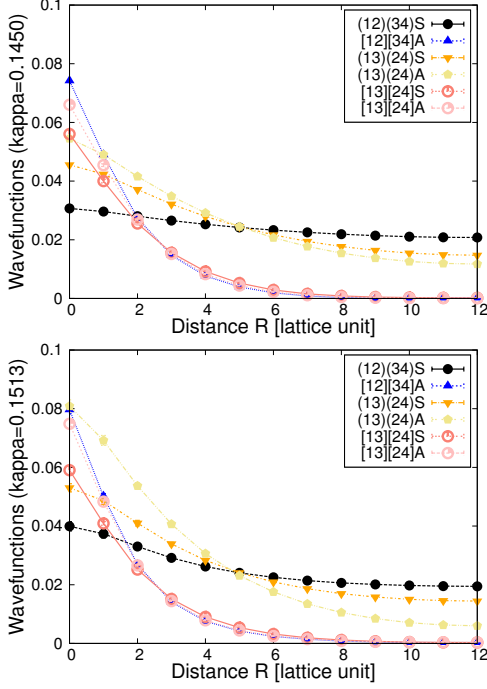


FIG. 4: All the wavefunctions are plotted as functions of distance  $R$  for  $\kappa = 0.1450$  and  $0.1513$ . They are normalized within  $0 \leq R \leq 7$ .

and  $(1,3)(2,4)A$  channels, wavefunctions remain finite at the asymptotic region, which shows that rearrangement of quarks is realized in hadron scatterings: Only a 4-quark state with  $(1,2)(3,4)S$  is created at  $t = 0$  (source point), and after (Euclidean) time evolution, quarks are exchanged among hadrons and other possible channels appear at the late Euclidean time. On the other hand, wavefunctions measured by colored operators ( $[1,2][3,4]A$ ,  $[1,3][2,4]S$  and  $[1,3][2,4]A$  channels) exponentially damp in the asymptotic region. These observations imply that colored diquarks cannot appear as asymptotic states, and are bounded at the short-distance region in hadron scatterings due to the color confinement. Such bounded colored diquarks form so-called “multi-quark” states.

In this paper, we especially concentrate on  $[1,2][3,4]A$  wavefunctions, which has no overlap with and is completely independent from incoming  $(1,2)(3,4)S$  state. In the channel, each diquark operator belongs to a color-triplet state and can be a probe for color excitations in hadron scatterings.

### C. Colored Wavefunctions

In Fig. 6, we again show the wavefunctions  $\Phi_{[12][34]A}(R)$  and  $\Phi_{[13][24]A}(R)$  from BS amplitudes as well as the squared internal wavefunctions,  $\Phi_{(12)S}(R)^2$  and  $\Phi_{(12)A}(R)^2$  for scalar- and axialvector diquarks.

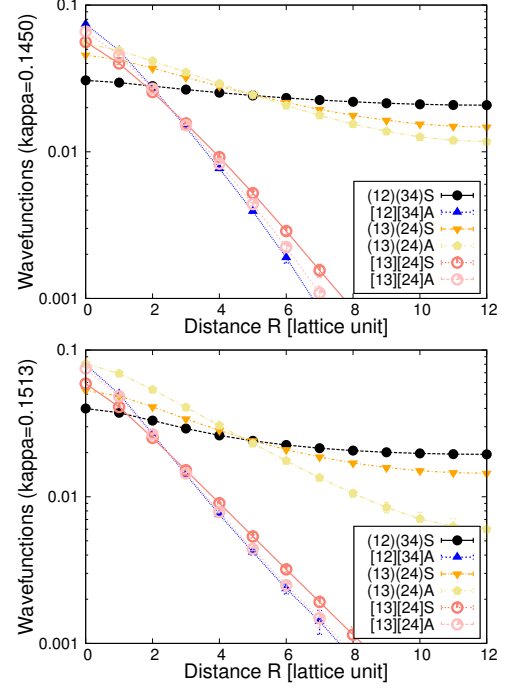


FIG. 5: All the wavefunctions are logarithmically plotted as functions of distance  $R$  for  $\kappa = 0.1450$  and  $0.1513$ . They are normalized within  $0 \leq R \leq 7$ .

All the wavefunctions are normalized within  $0 \leq R \leq 7$  to avoid possible finite-size effects at the boundary. As the quark mass decreases, the internal wavefunction of the axialvector diquark gets broader, while that of the scalar diquark shows little quark-mass dependence. The colored-diquark distributions,  $\Phi_{[12][34]A}(R)$  and  $\Phi_{[13][24]A}(R)$ , are remarkably enhanced at the short range for the larger  $\kappa$ , which implies color exchange among quarks is much more active for the lighter quark mass. This is consistent with the scenario proposed in Ref. [10]: The short-range attraction shows strong quark-mass dependence and may come from the color-magnetic interactions (color exchange).

We should note here that such color contributions evaluated from  $\Phi_{[12][34]A}(R)$  and  $\Phi_{[13][24]A}(R)$  do not always indicate the genuine OGE-origin colored-diquark components (genuine color excitations) but also include trivial colored two-quark contributions. It comes from the fact that all the colored-diquark components can be always expressed in terms of color-singlet degrees of freedom. For example,  $\Phi_{[12][34]A}(R)$ , extracted by two colored-diquark fields  $q_1(\mathbf{0})q_2(\mathbf{0})$  and  $q_3(\mathbf{R})q_4(\mathbf{R})$  with separation  $R$ , has non-zero overlap with color-singlet diquark scattering wavefunction  $|(13)S(24)S\rangle$ , which consists of two color-singlet diquarks  $|(13)S\rangle$  and  $|(24)S\rangle$ . Namely, taking into account that  $T_{ab}^c T_{a'b'}^c$  can be transformed by linear combination of  $\varepsilon_{aa'}\varepsilon_{bb'}$  and  $\varepsilon_{ab'}\varepsilon_{ba'}$ , the overlap is

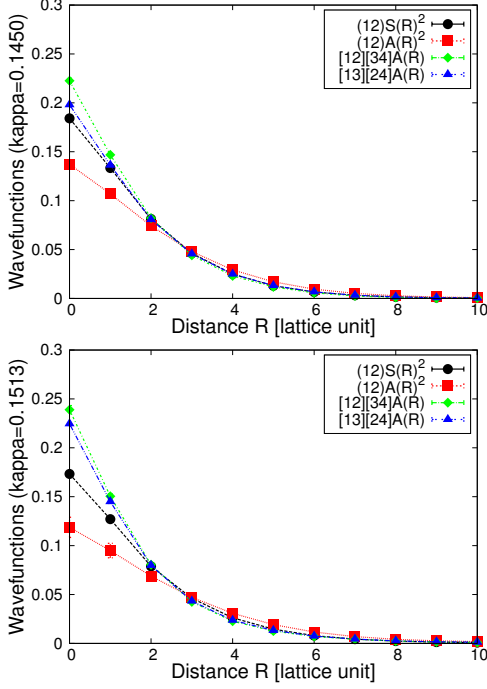


FIG. 6: The wavefunctions measured by colored operators as well as the squared wavefunctions of single hadrons, which are normalized within  $0 \leq R \leq 7$ , are plotted.

written as

$$\begin{aligned}
 & \sum_c \langle \text{vac} | \phi_{[12]A}^c(\mathbf{0}) \phi_{[34]A}^c(\mathbf{R}) | (13)S(24)S \rangle \\
 & \sim T_{ab}^c T_{a'b'}^c \langle \text{vac} | q_1^a(\mathbf{0}) q_2^b(\mathbf{0}) q_3^{a'}(\mathbf{R}) q_4^{b'}(\mathbf{R}) | (13)S \rangle \langle (24)S | \\
 & = T_{ab}^c T_{a'b'}^c \langle \text{vac} | q_1^a(\mathbf{0}) q_3^{a'}(\mathbf{R}) | (13)S \rangle \langle \text{vac} | q_2^b(\mathbf{0}) q_4^{b'}(\mathbf{R}) | (24)S \rangle \\
 & \sim \varepsilon_{aa'} \varepsilon_{bb'} \langle \text{vac} | q_1^a(\mathbf{0}) q_3^{a'}(\mathbf{R}) | (13)S \rangle \langle \text{vac} | q_2^b(\mathbf{0}) q_4^{b'}(\mathbf{R}) | (24)S \rangle \\
 & \sim \Phi_{(13)S}(R) \Phi_{(24)S}(R).
 \end{aligned} \tag{8}$$

Here we omit some normalization factors and consider the extreme case that the internal hadron structure does not change in the scattering. In such cases, the  $R$ -dependence of  $\Phi_{[12][34]A}(R)$  is expressed in terms of diquark (internal) wavefunctions. If  $\Phi_{[12][34]A}(R)$  is reflecting only the quark-rearranged color-singlet scattering waves  $|(13)(24)S\rangle$  or  $|(13)(24)A\rangle$ , its  $R$ -dependence will resemble those of squared internal wavefunctions,  $\Phi_{(12)S}(R)^2$  and  $\Phi_{(12)A}(R)^2$ , of color-singlet diquarks.

In order to compare colored-diquark distributions and color-singlet diquark (internal) wavefunctions, in terms of  $R$ -dependence, we show wavefunctions normalized by  $\Phi_{(12)S}(R)^2$  in Fig. 7. If there is no genuine colored-diquark component and  $\Phi_{[12][34]A}(R)$  simply reflects trivial colored two-quark contributions, the colored-diquark distribution functions  $\Phi_{[12][34]A}(R)$  and  $\Phi_{[13][24]A}(R)$  will show  $R$  dependences similar to  $\Phi_{(12)S}(R)^2$  and  $\Phi_{(12)A}(R)^2$  (possible two color-singlet degrees of freedom). In actuality, the colored-diquark distributions

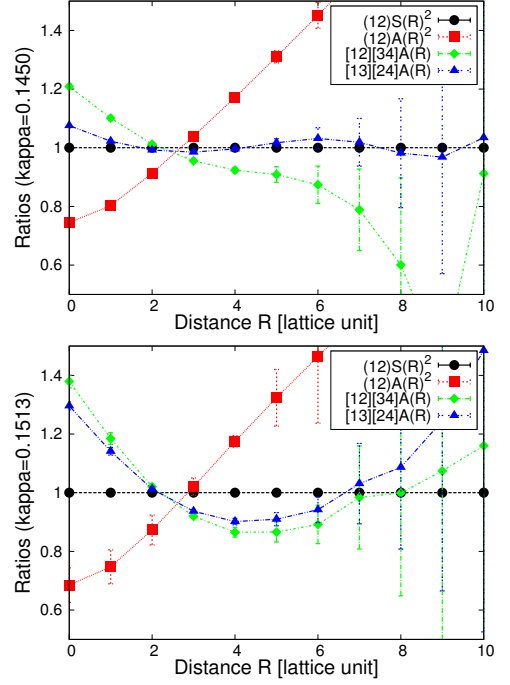


FIG. 7: Ratios between the wavefunctions from colored operators and the squared wavefunction of the scalar diquark hadron, which are normalized within  $0 \leq R \leq 7$ , are plotted.

$\Phi_{[12][34]A}(R)$  and  $\Phi_{[13][24]A}(R)$  at  $R < 2$  lie above those two lines. Especially  $\Phi_{[12][34]A}(R)$  clearly lies above  $\Phi_{(12)S}(R)^2$ , and this tendency is stronger at lighter quark mass region. Then, enhanced color excitations are expected at  $R < 2$ . In the case of  $\Phi_{[13][24]A}(R)$ , it is relatively smaller. The reason is the asymmetry between  $(12)(34)S$  and  $(13)(24)S$  asymptotic states. At the source point, only  $(12)(34)S$  state is created and this leads to the relative suppression of  $(13)(24)S$  waves. While  $\Phi_{[13][24]A}(R)$  would surely contain colored-diquark contribution, it is smaller because of the suppression of  $(13)(24)S$  incoming waves, and it largely reflects the trivial colored two-quark components from the (relatively larger) incoming and outgoing  $(12)(34)S$  state.

## IV. ADDITIONAL ANALYSES

### A. Isolating color excitations

QCD interactions may be classified into two categories. One is highly nonperturbative dynamics, which leads to the chiral-symmetry breaking, color confinement and etc, and the other is perturbative contributions represented by one gluon exchange (OGE) interactions among quarks. These two distinct phenomena originate from difference energy scales. A method that restricts energy scale of gluons via the Fourier transformation was pro-



posed and tested [26, 27].

One of the principal origins of color excitations would be high-energy gluon exchanges (one gluon exchange) at the short-distance regions. When a gluon is exchanged between 1- and 3-quarks in the (12)(34)S hadronic state, a [12][34]A state would be formed as an intermediate state. As discussed before, the [12][34]A component measured by colored-diquark operators cannot be fully distinguished from (13)(24)S or (14)(23)S hadronic states, since (13)(24)S and (14)(23)S states can be asymptotic states and are mixed in hadronic scattering to contribute to the colored-diquark components. In order to make (13)(24)S and (14)(23)S asymptotic states absent from the system and isolate color excitations, we make high-momentum gluons be common among all the quarks, and let low-momentum gluons be independent. If low-momentum gluons are made common between 1,2 and 3,4 quarks, only the (12)(34)S asymptotic state survives but asymptotic states of other channels (13)(24)S or (14)(23)S are prohibited, since confining force always acts only between 1,2 and 3,4 quarks. (Not between 1,3 and 2,4 quarks.)

After this gluon-manipulation, the asymptotic region of the system is fulfilled only by (12)(34)S diquark scattering waves and  $\Phi_{[12][34]A}(R)$  does not contain contaminations from (13)(24)S and (14)(23)S scattering wavefunctions.

With this aim, we generate three different series of SU(2) link variables (gluon fields),  $U_\mu(\mathbf{x}, t; C)$ ,  $U_\mu(\mathbf{x}, t; C')$  and  $U_\mu(\mathbf{x}, t; C'')$ . We perform 3-dim Fourier transformation [28] for link variables  $U_\mu(\mathbf{x}, t)$  in the Landau gauge and extract  $U_\mu(\mathbf{p}, t)$  in momentum space:

$$U_\mu(\mathbf{p}, t) = \sum_{\mathbf{x}} U_\mu(\mathbf{x}, t) e^{i\mathbf{p} \cdot \mathbf{x}} \quad (9)$$

We divide link variables into low- and high-momentum contributions,

$$\tilde{U}_\mu^L(\mathbf{p}, t) = U_\mu(\mathbf{p}, t) \quad (|\mathbf{p}| \leq \Lambda) \quad (10)$$

$$\tilde{U}_\mu^H(\mathbf{p}, t) = U_\mu(\mathbf{p}, t) \quad (|\mathbf{p}| \geq \Lambda) \quad (11)$$

and construct mixed link variables as

$$\tilde{U}_\mu(\mathbf{p}, t; C_A) = \tilde{U}_\mu^L(\mathbf{p}, t; C') + \tilde{U}_\mu^H(\mathbf{p}, t; C) \quad (12)$$

$$\tilde{U}_\mu(\mathbf{p}, t; C_B) = \tilde{U}_\mu^L(\mathbf{p}, t; C'') + \tilde{U}_\mu^H(\mathbf{p}, t; C) \quad (13)$$

With link variables reconverted into the coordinate representation,

$$\tilde{U}_\mu(\mathbf{x}, t) \equiv \frac{1}{V} \sum_{\mathbf{p}} \tilde{U}_\mu(\mathbf{p}, t) e^{-i\mathbf{p} \cdot \mathbf{x}}, \quad (14)$$

which no longer belong to SU(2), new SU(2) link variables in the coordinate space  $U_\mu(\mathbf{x}, t)$  are reconstructed so that the distance,

$$\text{Tr} (U_\mu(\mathbf{x}, t) - \tilde{U}_\mu(\mathbf{x}, t))(U_\mu(\mathbf{x}, t) - \tilde{U}_\mu(\mathbf{x}, t))^\dagger, \quad (15)$$

is minimized. The infrared(IR) cut  $\Lambda$  is set to  $\Lambda = 5$  in lattice unit (about 1 GeV in the physical unit). 1,2-quarks' propagators are computed with thus constructed link variables  $U_\mu(\mathbf{x}, t; C_A)$ , and for 3,4-quarks' propagators we use  $U_\mu(\mathbf{x}, t; C_B)$ . Then,  $U_\mu(\mathbf{x}, t; C_A)$  and  $U_\mu(\mathbf{x}, t; C_B)$ , give independent low-energy QCD dynamics to 1,2-quarks and 3,4-quarks but high-momentum dynamics are common in all the quarks. Hadrons interacting with  $U_\mu(\mathbf{x}, t; C_A)$  and  $U_\mu(\mathbf{x}, t; C_B)$  have nothing to do with each other in the asymptotic region, but can exchange only high-momentum gluons in the short-distance region. Using this nature, we may single out color exchanges in the short-distance region; we do not suffer from the trivial colored two-quark state coming from transformation of hadronic basis. (Asymptotic two-hadron states in the (13)(24) and (14)(23) channels are prohibited since  $U_\mu(\mathbf{x}, t; C_A)$  and  $U_\mu(\mathbf{x}, t; C_B)$  give different confining forces.) Note that we also performed Fourier transformation in the Coulomb gauge and obtained qualitatively the same results.

## B. Isolated color excitations

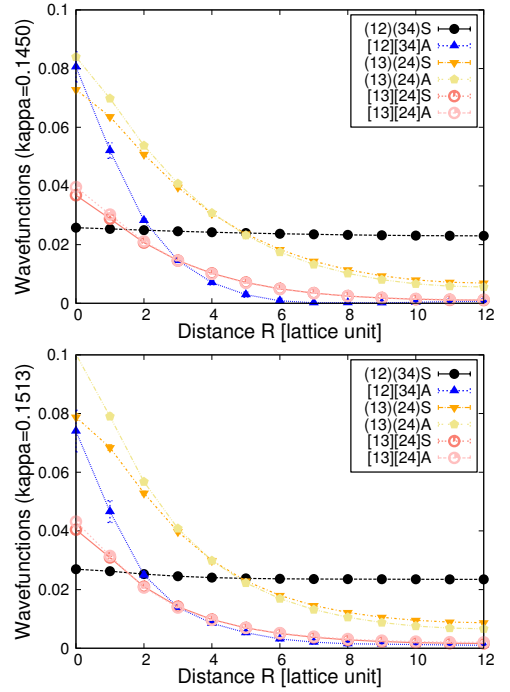


FIG. 8: All the wavefunctions, which are obtained without IR-gluon exchanges, are plotted as functions of distance  $R$  for  $\kappa = 0.1450$  and  $0.1513$ . They are normalized within  $0 \leq R \leq 7$ .

In Fig.8 and 9, the wavefunctions obtained in this framework are displayed. 1, 2-quarks and 3, 4-quarks belong to different low-energy QCD dynamics but their high-energy dynamics are common and high-momentum

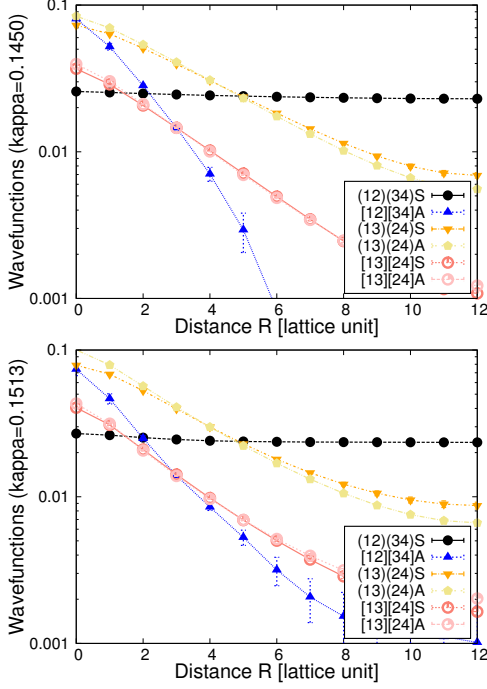


FIG. 9: All the wavefunctions, which are obtained without IR-gluon exchanges, are logarithmically plotted as functions of distance  $R$  for  $\kappa = 0.1450$  and  $0.1513$ . They are normalized within  $0 \leq R \leq 7$ .

gluons can be exchanged among these four quarks.

At the source, a  $(1,2)(3,4)S$ -state are created and even at the large Euclidean time only the  $(1,2)(3,4)S$ -state can be observed in the asymptotic region, which implies that asymptotic two-hadron states in other flavor channels are successfully prohibited. All the other wavefunctions exponentially damp at large  $R$ . On the other hand, wavefunctions for  $[1, 2][3, 4]A$ ,  $[1, 3][2, 4]S$  and  $[1, 3][2, 4]A$  channels exponentially damp toward the asymptotic region, which remains unchanged as compared to the previous analyses.

In Fig. 10 and 11, squared internal wavefunctions,  $\Phi_{(12)S}(R)^2$  and  $\Phi_{(12)A}(R)^2$  for scalar- and axialvector diquarks, and relative wavefunctions,  $\Phi_{[12][34]A}(R)$  and  $\Phi_{[13][24]A}(R)$ , are plotted. All the wavefunctions are normalized within  $0 \leq r \leq 7$ . The colored contributions  $\Phi_{[12][34]A}(R)$  remains unchanged and is remarkably enhanced again at the short range for the larger  $\kappa$ . Now that  $(13)(24)S$  and  $(14)(23)S$  asymptotic scattering waves do not exist, “color excitation” measured by  $\Phi_{[12][34]A}(R)$  is safe from trivial colored contaminations from asymptotic scattering states. We can conclude that  $\Phi_{[12][34]A}(R)$  around the origin mainly originates from genuine color excitation modes.

On the other hand,  $\Phi_{[13][24]A}(R)$  does not show the short-range enhancement and lie between  $\Phi_{(12)S}(R)^2$  and  $\Phi_{(12)A}(R)^2$ , which implies that  $\Phi_{[13][24]A}(R)$  in the present analysis little contains genuine color excitation

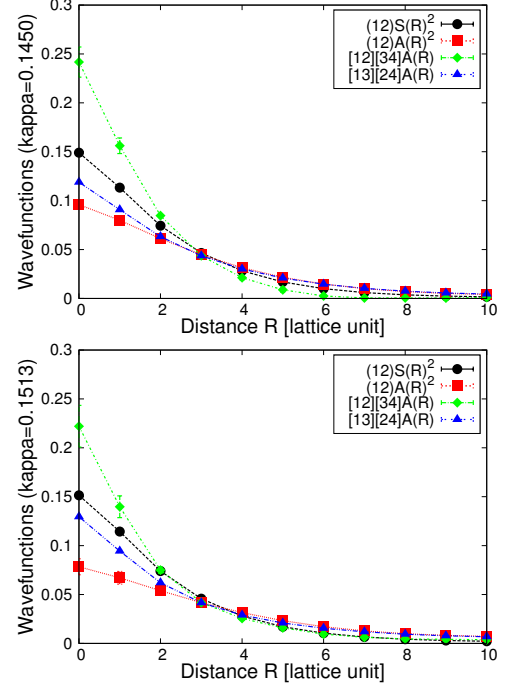


FIG. 10: The wavefunctions measured by colored operators as well as the squared wavefunctions of single hadrons, are plotted. They are obtained without IR-gluon exchanges and are normalized within  $0 \leq R \leq 7$ , are plotted.

components. The reason for that is the suppression of incoming and outgoing  $(13)(24)S$  and  $(14)(23)S$  scattering waves: If  $(13)(24)S$  incoming amplitude is absent, the magnitude of color-excited  $\{13\}\{24\}A$  state will be inevitably suppressed. Then  $\Phi_{[13][24]A}(R)$  mainly contains trivial colored state from the incoming and outgoing  $(12)(34)S$  scattering waves, which is not suppressed in this analysis.

## V. DISCUSSIONS

We have found so far that

- The enhancement of  $\Phi_{[13][24]A}(R)$  at the short range shows the manifestation of the color excitation modes in hadron scattering.
- The color excitation modes much more appear when quark masses are lighter.
- The color-excitation is intense at  $R < 2$  in the lattice unit ( $R < 0.2$  fm).

We here discuss the physical implication of the short-range color excitations caused by ultraviolet(UV)-gluon exchanges. When two color-singlet hadrons gets close to each other, color-excited (multi-quark) states are formed

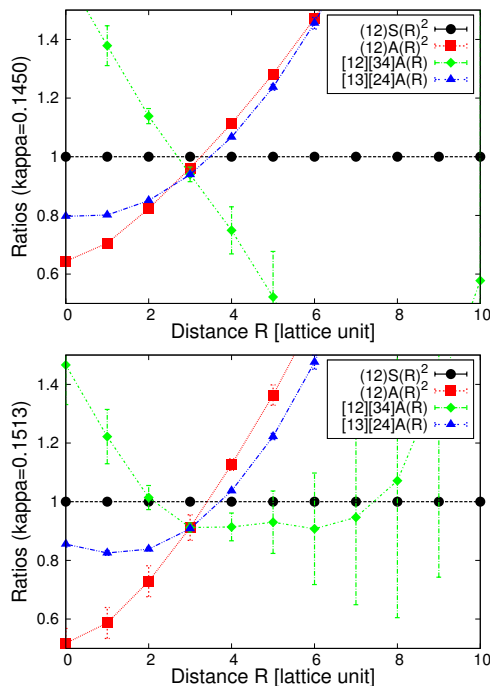


FIG. 11: Ratios between the wavefunctions from colored operators and the squared wavefunction of the scalar diquark hadron, which are normalized within  $0 \leq R \leq 7$ , are plotted. They are obtained without IR-gluon exchanges.

exchanging UV gluons. This color excitations eventually cause short-range attractive force among hadrons reported in Ref. [10]. To see this, we construct hadronic potentials from two-hadron wavefunctions assuming nonrelativistic Schrödinger equations. The reconstructed potentials for  $(12)(34)S$  scattering channel with and without IR-gluon exchanges are shown in Fig.12. The potential for  $(12)(34)S$  channel with IR-gluon exchanges is nothing but the attractive potential for the direct diagram  $V_{\text{dir}}$  found in our previous work [10].

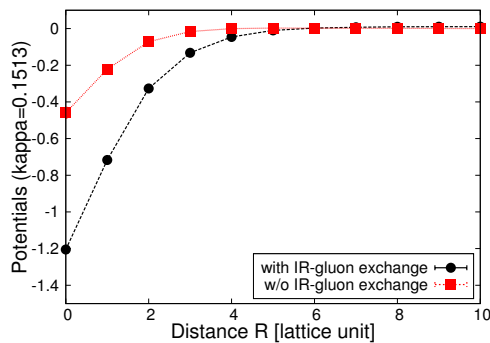


FIG. 12: Reconstructed potentials for  $(12)(34)S$  channel at  $\kappa = 0.1513$ . The circles are the potential obtained by the full gluon dynamics and the squares are that obtained without IR-gluon exchanges.

Even when IR-gluon exchanges are made inactivated, an attractive potential appears between two singlet hadrons, which can be seen as the dips around the origin. We fit the potential with an single-exponential function  $V(R) = -A \exp(-BR)$ , with  $A$  and  $B$  being a strength and a range parameters. (Such attractive potentials will include universal long-range attractive potential  $V_{\text{att}}^U(R)$  [10]. Since its contribution is smaller in lighter quark-mass and short-distance region, it is neglected in this analysis;  $V(R) = V_{\text{dir}}(R) \sim V_{\text{att}}^D(R) \equiv V_{\text{dir}}(R) - V_{\text{att}}^U(R)$ .) We plot in Fig. 13 the fitted parameters as functions of the half of the axial-vector diquark mass. The parameters without IR-gluon exchanges are labeled as “ $(12)(34)S$  w/o IR-gluon exchange”. Though the strength itself decreases without IR-gluon exchanges, the interaction ranges are almost independent from quark masses and those obtained with and without IR gluons are consistent with each other. (When IR-gluon exchange between  $(12)$ -diquark and  $(34)$ -diquark is cut, the energies of color combinations other than  $(12)(34)$ , including genuine 4-quark states etc., are all raised, which may have caused the reduced strength.) The interaction range is about 1 in the lattice unit and it is identified as the shortest-range attractive interaction  $V_{\text{att}}$  observed in our previous work [10]. Taking into account that 12- and 34-diquarks do not exchange low-energy gluons and non-perturbative interactions between 12- and 34-diquarks is absent, this observation implies that the shortest-range gluon interaction mainly creates colored-diquark states as intermediate states and gives rise to the shortest-range attractive potential.

## VI. SUMMARY AND OUTLOOKS

We have computed colored-diquark distributions in two-hadron scatterings using color SU(2) lattice QCD by means of Bethe-Salpeter amplitudes on the lattice. Using colored-diquark operators in the Coulomb gauge, we have directly measured colored-diquark components produced via one gluon exchange (OGE) processes in hadron scattering. As a result, we have found that the colored-diquark components are much enhanced at the short range,  $< 0.2$  fm, and that their  $R$ -dependence shows the tail described well by a single-exponential function.

We have repeated the analyses on the artificially constructed gauge fields, where low- and high-momentum gluon components are decoupled and only restricted pair of quarks can share low-momentum gluons, so that we can distinguish the genuine colored-diquark components from possible trivial colored two-quark components contained in two color-singlet hadrons as a result of simple transformation of hadronic basis. Qualitatively the same behavior is actually found on this analysis, and it is confirmed that the enhancement of the colored-diquark distribution at the short range we have observed is genuine OGE-origin color excitation. We have also estimated the quark-mass dependence of the color-exchange range, and



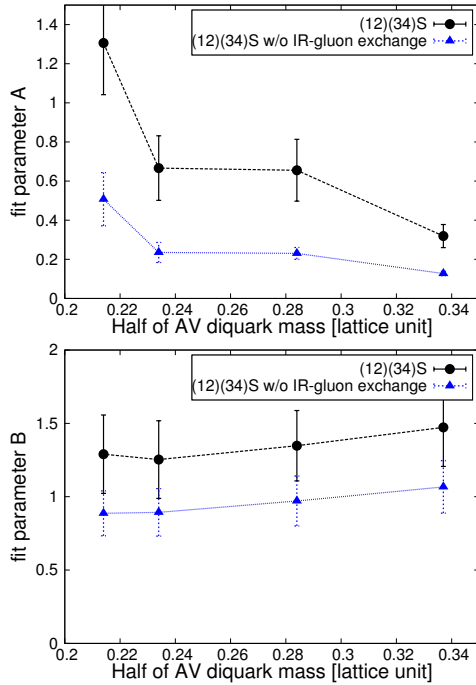


FIG. 13: Fitting parameters for the  $(12)(34)S$  potentials obtained with and without IR-gluon exchanges. The potentials are fitted by  $V = -A \exp(-Br)$ . The upper panel shows the strength  $A$ , and the lower panel the interaction range  $B$ . The horizontal axes denote the half of axial vector diquark mass at each  $\kappa$ .

the results imply that the shortest-ranged attractive force found in two-hadron scatterings is originated from the OGE processes between hadrons.

The short-range color-exchange processes produce colored many-quark objects and enable quarks to move from one hadron to another. One of the intriguing corresponding phenomena may include so-called quarkyonic phase [15–21]. In a cold high density matter, quark's degrees of freedom are expected to be manifested at a certain density despite of its color-confining nature [14–21]. In such a system, hadrons are closely located each other and the enhanced short-range OGE processes would make hadrons colored. This color percolation enables quarks to move from one to another. To cast light on such phenomena from the view point of quarks and gluons, the much more clarification of color exchanges among hadrons at high density can be one of the important keys.

### Acknowledgments

All the numerical calculations were performed on NEC SX-8R at CMC, Osaka university, on SX-8 at YITP, Kyoto University. This work was supported in part by the Yukawa International Program for Quark-Hadron Sciences (YIPQS), and the Grant-in-Aid for the Global COE Program “The Next Generation of Physics, Spun from Universality and Emergence” from MEXT of Japan, and by KAKENHI (21740181, 25247036, 26400270).

- 
- [1] H. Yukawa, Proc. Phys. Math. Soc. Jap. **17**, 48 (1935).
  - [2] Prog. Theor. Phys. Suppl. **39** (1967).
  - [3] Rev. Mod. Phys. **39**, p495 (1967).
  - [4] R. Machleidt, K. Holinde and C. Elster, Phys. Rept. **149**, 1 (1987).
  - [5] M. Oka and K. Yazaki, Phys. Lett. B **90**, 41 (1980).
  - [6] M. Oka and K. Yazaki, Prog. Theor. Phys. **66**, 556 (1981).
  - [7] M. Oka and K. Yazaki, Prog. Theor. Phys. **66**, 572 (1981).
  - [8] N. Ishii, S. Aoki and T. Hatsuda, Phys. Rev. Lett. **99**, 022001 (2007) [arXiv:nucl-th/0611096].
  - [9] S. Aoki *et al.* [HAL QCD Collaboration], PTEP **2012**, 01A105 (2012) doi:10.1093/ptep/pts010 [arXiv:1206.5088 [hep-lat]].
  - [10] T. T. Takahashi and Y. Kanada-En'yo, Phys. Rev. D **82**, 094506 (2010) doi:10.1103/PhysRevD.82.094506 [arXiv:0912.0691 [hep-lat]].
  - [11] M. Harvey, Nucl. Phys. A **352**, 326 (1981).
  - [12] F. Okiharu, H. Suganuma and T. T. Takahashi, Phys. Rev. D **72**, 014505 (2005) [arXiv:hep-lat/0412012].
  - [13] F. Okiharu, H. Suganuma and T. T. Takahashi, Phys. Rev. Lett. **94**, 192001 (2005) doi:10.1103/PhysRevLett.94.192001 [hep-lat/0407001].
  - [14] G. Baym and S. A. Chin, Phys. Lett. B **62**, 241 (1976). doi:10.1016/0370-2693(76)90517-7
  - [15] L. McLerran and R. D. Pisarski, Nucl. Phys. A **796**, 83 (2007) doi:10.1016/j.nuclphysa.2007.08.013 [arXiv:0706.2191 [hep-ph]].
  - [16] H. Abuki, R. Anglani, R. Gatto, G. Nardulli and M. Ruggieri, Phys. Rev. D **78**, 034034 (2008) doi:10.1103/PhysRevD.78.034034 [arXiv:0805.1509 [hep-ph]].
  - [17] K. Miura, T. Z. Nakano and A. Ohnishi, Prog. Theor. Phys. **122**, 1045 (2009) doi:10.1143/PTP.122.1045 [arXiv:0806.3357 [nucl-th]].
  - [18] L. McLerran, K. Redlich and C. Sasaki, Nucl. Phys. A **824**, 86 (2009) doi:10.1016/j.nuclphysa.2009.04.001 [arXiv:0812.3585 [hep-ph]].
  - [19] T. Brauner, K. Fukushima and Y. Hidaka, Phys. Rev. D **80**, 074035 (2009) Erratum: [Phys. Rev. D **81**, 119904 (2010)] doi:10.1103/PhysRevD.81.119904, 10.1103/PhysRevD.80.074035 [arXiv:0907.4905 [hep-ph]].
  - [20] S. Hands, S. Kim and J. I. Skullerud, Phys. Rev. D **81**, 091502 (2010) doi:10.1103/PhysRevD.81.091502 [arXiv:1001.1682 [hep-lat]].
  - [21] K. Fukushima and T. Kojo, Astrophys. J. **817**, no. 2, 180 (2016) doi:10.3847/0004-637X/817/2/180 [arXiv:1509.00356 [nucl-th]].
  - [22] S. Aoki *et al.* [CP-PACS Collaboration], Phys. Rev. D **71**, 094504 (2005) [arXiv:hep-lat/0503025].

- [23] S. Aoki, T. Hatsuda and N. Ishii, Prog. Theor. Phys. **123**, 89 (2010) [arXiv:0909.5585 [hep-lat]].
- [24] J. Fingberg, U. M. Heller and F. Karsch, Nucl. Phys. B **392**, 493 (1993) [arXiv:hep-lat/9208012].
- [25] J. D. Stack, S. D. Neiman and R. J. Wensley, Phys. Rev. D **50**, 3399 (1994) [arXiv:hep-lat/9404014].
- [26] A. Yamamoto and H. Suganuma, Phys. Rev. Lett. **101**, 241601 (2008) [arXiv:0808.1120 [hep-lat]].
- [27] A. Yamamoto and H. Suganuma, Phys. Rev. D **79**, 054504 (2009) [arXiv:0811.3845 [hep-lat]].
- [28] A. Yamamoto, Phys. Lett. B **688**, 345 (2010) doi:10.1016/j.physletb.2010.04.022 [arXiv:0906.2618 [hep-lat]].